Society for Mathematical Biology

ORIGINAL ARTICLE



The implications of host–pathogen co-evolutionary outcomes on macro-epidemics based on a combined-host strategy

Qiutong Liu¹ · Yanni Xiao¹ · Stacey R. Smith?²

Received: 25 December 2024 / Accepted: 12 August 2025 / Published online: 10 September 2025 © The Author(s), under exclusive licence to the Society for Mathematical Biology 2025

Abstract

Host defense and pathogen virulence interact and mutually shape each other's evolution. Host–pathogen co-evolutionary outcomes have potentially significant impacts on population dynamics and vice versa. To investigate host–pathogen interactions and explore the impact of micro-level co-evolutionary outcomes on macro-level epidemics, we develop a co-evolutionary model with a combined host-defense strategy. Our results illustrate that host–pathogen co-evolution may induce infection cycling and lead to the vanishing of the disease-induced hydra effect, whereas pathogen monoevolution strengthens the hydra effect in both range and magnitude. As the recovery rate increases, we find a counter-intuitive effect of increased disease prevalence due to host–pathogen co-evolution: the disease is first highly infectious and lethal, then highly infectious but with low lethality. Such diverse outcomes suggest that this combined co-evolutionary and epidemiological framework holds great promise for a better understanding of infection.

Keywords Host–pathogen co-evolution · Infection cycling · Transmission patterns · Hydra effect

1 Introduction

In species with antagonistic interactions, such as in host-pathogen systems, coevolution is recognized as one of the most significant processes in creating and

- ✓ Yanni Xiao yxiao@mail.xjtu.edu.cn
- Stacey R. Smith? stacey.smith@uottawa.ca

Qiutong Liu lqt19971018@stu.xjtu.edu.cn

- School of Mathematics and Statistics, Xi'an Jiaotong University, Xi'an 710049, PR China
- Department of Mathematics and Faculty of Medicine, The University of Ottawa, Ottawa, ON K1N 6N5, Canada



maintaining species diversity (Mougi and Iwasa 2010). Typically, host–pathogen interactions have strong effects on individual fitness and can significantly alter the evolutionary trajectory of species; conversely, evolutionary outcomes can affect host–pathogen populations (Tibayrenc 2024; Buckingham and Ashby 2022; Simmonds et al. 2019; Yang et al. 2022). These factors suggest that for an accurate understanding of infectious diseases, host–pathogen co-evolutionary processes need to be understood in epidemiological contexts. Experimental studies of host–pathogen co-evolutionary processes have recently gained increasing attention from biologists, epidemiologists and mathematical modellers (Lopez-Pascua and Buckling 2008; Bonachela 2024; Hall et al. 2011; Gómez and Buckling 2011; Castledine et al. 2022), but demonstrating co-evolutionary mechanisms of host–pathogen interactions remains difficult and is one of the key challenges for evolutionary biology.

Pathogens can be a primary source of host selection by shortening host lifespan or reducing their fertility (Restif and Koella 2004); conversely, the host can shape pathogen evolution (Simmonds et al. 2019). Hosts have evolved various defense mechanisms to reduce the damaging effects of infection. These defenses — which may depend on the immune system, cell surface modifications, changes in behaviour or life-history strategies — generally fall into two distinct categories: resistance, which reduces the pathogen load (Boots and Bowers 1999; Malo and Skamene 1994), and tolerance, which ameliorates the damage that a pathogen causes to its host, without reducing the pathogen load (Boots et al. 2009; Vitale and Best 2019). Hosts can evolve a wide range of resistance mechanisms in response to pathogens, which can be functionally classified as avoidance, increased recovery and reduced pathogen replication rate (Boots et al. 2009; Miller et al. 2007). Tolerance, on the other hand, is primarily classified based on its effect on reducing the pathogen's impact on host mortality or reproduction (Restif and Koella 2004; Best et al. 2017). A key assumption in almost all theoretical evolutionary studies is that adaptive defense is costly, and host defenses increase at the expense of other traits (Boots et al. 2009; Vitale and Best 2019; Cressler et al. 2015; Antonovics and Thrall 1994), such as fecundity, with both theoretical arguments and empirical evidence (Yang et al. 2022; Boots et al. 2009; Bartlett et al. 2018; Best et al. 2015; Gascuel et al. 2013). Theoretical studies on the evolution of pathogens typically assume a trade-off between mortality and transmission, known as the mortality-transmission trade-off (Yang et al. 2022; Bull and Lauring 2014; Liu and Xiao 2023). According to this trade-off theory, a pathogen cannot simultaneously increase its transmission and prolong infection; in other words, host mortality constrains transmission. As a result, pathogens aim to maximize their fitness while being subject to these costs, a concept that has been empirically supported (Doumayrou et al. 2013).

A number of different modelling approaches have been developed to study evolutionary mechanisms, such as quantitative genetic methods, locus-based methods and adaptive dynamics (Boots et al. 2009; Iwasa et al. 1991). The study of long-term dynamics is of great significance for epidemiology, and the adaptive-dynamics approach allows us to examine long-term evolutionary factors (Dieckmann and Law 1996; Geritz et al. 1998; Metz et al. 1992). The long-term behavior of host–pathogen interactions is directly linked to the interplay between evolutionary traits of both species, known as co-evolutionary dynamics (Yang et al. 2022; Boots et al. 2009; Best



et al. 2009). Given the limited empirical research on co-evolution, here we consider the question: can modelling host–pathogen co-evolution on the micro scale produce tangible outcomes on the macro scale?

Mathematical models have been applied to explore the evolution of single phenotypic traits; namely, pathogen virulence (Liu and Xiao 2023; Alizon et al. 2009; Boldin and Diekmann 2008) or defense in the form of resistance or tolerance (Vitale and Best 2019; Gascuel et al. 2013; Hulse et al. 2023; Singh and Best 2023; Bonneaud et al. 2019). However, host–pathogen interactions are generally co-evolutionary processes in nature (Simmonds et al. 2019; Yang et al. 2022; Woolhouse et al. 2002), and the co-evolutionary dynamics of quantitative traits in both host and pathogen is rarely investigated. Previous studies on host-pathogen co-evolution mainly considered pure host strategies; i.e., either resistance or tolerance (Yang et al. 2022; Best et al. 2009; Hulse et al. 2023; McLeod and Day 2015; Best et al. 2011). In practice, however, host defense involves both resistance and tolerance (Liu et al. 2020; McCarville and Ayres 2018; Singh and Best 2021), and empirical studies have found both defense mechanisms present within a single population (Stowe 1998; Carmona and Fornoni 2013; Núñez-Farfán et al. 2007). Population dynamics are intrinsically linked to evolutionary dynamics, forming an eco-evolutionary feedback (Post and Palkovacs 2009) and enabling modelling of more complex biological scenarios, such as evolutionary cycling (Mougi and Iwasa 2010; Buckingham and Ashby 2022; Yang et al. 2022; Ashby et al. 2019). Host-pathogen co-evolutionary cycling has been observed experimentally (Hall et al. 2011; Decaestecker et al. 2007), which is a crucial effect of maintaining diversity (Buckingham and Ashby 2022). Disease prevalence could be influenced by evolution, potentially leading to disease reversal that may compromise the effectiveness of prevention and control methods (Singh and Best 2023), but the relevant literature in the context of host-pathogen co-evolution is scarce. The paradoxical effect of increasing population density due to the introduction of a disease is termed the disease-induced hydra effect (Jaramillo et al. 2022). To the best of our knowledge, no modelling study has yet considered the impact of co-evolutionary effects on such hydra effects.

Here, we aim to investigate the co-evolutionary dynamics of combined host defense (resistance and tolerance) and pathogen virulence to describe host–pathogen interactions and, in turn, explore the impact of micro-level evolutionary outcomes on macro-level epidemics and vice versa. Based on the adaptive-dynamics framework and simulations of the co-evolutionary model, we determine conditions where host and pathogen phenotypic traits co-evolve into a continuous stable strategy or periodic cycling. Specifically, we examine disease-reversal phenomena and disease-induced hydra effects in various evolutionary contexts.

The rest of our paper is organized as follows. In Section 2, we formulate the epidemiological model and classify the existence of equilibria and investigate their stability. We then analyze the existence of the disease-induced hydra effect in our model in the absence of evolution. In Section 3, using the approach of adaptive dynamics, we analyze the co-evolutionary invasion process of host defense and pathogen virulence, and we propose a corresponding co-evolutionary model. In Section 4, numerical simulations are performed to illustrate how co-evolutionary adaptation affects the dynamic behaviour of population size and trait values. We conclude with a discussion.



148 Page 4 of 28 Q. Liu et al.

2 Epidemiological model

We assume that there is only one monomorphic host type and one monomorphic pathogen type in the initial community. The host population is regulated by intraspecific competition for resources, and we hypothesize that the population birth rate is a density-dependent function and that infection could affect reproduction and intraspecific competition. We assume that the pathogen can cause direct transmission without latency and that the incidence of host infection is bilinear. Infected individuals can recover, but recovery does not provide immunity. These assumptions form an extended model based on the classic host–pathogen structure (Anderson and May 1981). The population dynamics of the host–pathogen interaction are given by

$$\frac{dS}{dt} = b(S + \tau_1 I)F(S + \tau_2 I) - \beta SI - dS + \gamma I,
\frac{dI}{dt} = \beta SI - (\alpha + d + \gamma)I.$$
(1)

Here, the variables S(t) and I(t) represent the numbers of susceptible and infectious individuals at time t, respectively. We model disease transmission using mass-action incidence βSI . β denotes the transmission rate, α represents the disease-induced death rate, and γ is the recovery rate. The term $bF(S+\tau_2I)$ is the density-dependent birth rate, and b is the per-capita birth rate. The parameter τ_1 denotes the fecundity of infected individuals compared to susceptible individuals, and τ_2 represents their relative ability to compete for resources, where $\tau_1, \tau_2 \in [0, 1]$. This assumption implies that infection could prevent reproduction and intra-specific competition. We further assume that $\tau_1 = \tau_2 = \tau$ for simplicity; that is, reductions in recruitment and resource competition for infectious individuals are the same. Specifically, $\tau = 1$, $\tau = 0$ and $\tau \in (0, 1)$ respectively indicate that the disease has no effect, completely inhibits or partially inhibits the recruitment of infected individuals. The function F(X) satisfies F'(X) < 0, $bF(\infty) < d$ and the intrinsic growth rate bF(0) > d, where d is the natural death rate. We further take $F(S+\tau I) = 1 - q(S+\tau I)$ throughout this paper, where q models the crowding effect on births. All parameters in model (1) are positive.

Note that the recruitment function bXF(X) is a downward-facing quadratic function in X, and hence there exists a maximum value b/(4qd) > bXF(X). Denote N(t) = S(t) + I(t). We obtain

$$\frac{dN}{dt} = b(S + \tau I)F(S + \tau I) - dN - \alpha I \le \frac{b}{4a} - dN,$$

which yields

$$\lim_{t\to\infty}\sup N(t)\leq \frac{b}{4qd}.$$

The feasible region for (1) is $\mathcal{D} = \{(S, I) \in \mathbb{R}^2_+ : S + I \leq \frac{b}{4ad}\}$.



2.1 Existence and stability of the ecological equilibria

In the following, we focus on the feasibility and stability of the equilibria of system (1).

Theorem 1 The boundary equilibrium $E_{00} = (0,0)$ of system (1) is always feasible and unstable. The disease-free equilibrium $E_0(S_0, I_0) = (\frac{b-d}{bq}, 0)$ of system (1) is always feasible under the assumption b > d and is locally asymptotically stable when $R_0 < 1$, where

$$R_{0} = \frac{\beta S_{0}}{\alpha + d + \gamma}, \quad S^{*} = \frac{\alpha + d + \gamma}{\beta},$$

$$I^{*} = \begin{cases} \frac{(\alpha + d + \gamma)(b(\beta - q(\alpha + d + \gamma)) - \beta d)}{\beta^{2}(\alpha + d)}, & \tau = 0\\ \frac{b\tau(1 - 2qS^{*}) - \alpha - d + \sqrt{\triangle}}{2b\tau^{2}q}, & \tau \in (0, 1], \end{cases}$$

with $\Delta = (b\tau(1-2qS^*) - \alpha - d)^2 + 4b\tau^2q(bS^*(1-qS^*) - dS^*)$. When $R_0 > 1$, the unique endemic equilibrum $E(S^*, I^*)$ of system (1) exists, and E is locally asymptotically stable.

The proof is presented in Appendix A. Here, R_0 is the basic reproduction number, which denotes the expected number of secondary cases produced in a completely susceptible population by a typical infected individual during their entire infectious period (Heffernan et al. 2005). Next, we discuss the global asymptotic stability of the ecological equilibria at specific values of τ .

Theorem 2 If $\tau = 0$, the disease-free equilibrium E_0 and the endemic equilibrium E of system (1) are globally asymptotically stable when the basic reproduction number $R_0 < 1$ and $R_0 > 1$, respectively. If $\tau = 1$, the disease-free equilibrium E_0 of system (1) is globally asymptotically stable when $R_0 < 1$.

The proof is presented in Appendix B.

2.2 The disease-induced hydra effect

A model with an asymptotically stable endemic equilibrium has a disease-induced hydra effect if the endemic population size $(N^* = S^* + I^*)$ is greater than the disease-free population size (S_0) for some values of the basic reproduction number $R_0 > 1$. We found that a disease-induced hydra effect could arise in epidemiological model (1), as shown in Fig. 1(a). This is further described in the following theorem.

Theorem 3 Suppose $R_0 > 1$. At the stable endemic equilibrium (S^*, I^*) , one of the following conditions is required to guarantee the existence of a disease-induced hydra effect in system (I):

- (1) For $\tau = 0$, the sufficient and necessary condition is $\frac{d}{dS^*}[S^*F(S^*)] < -\frac{\alpha}{b}$;
- (2) For $\tau \in (max\{0, \tau_b\}, \tau_t)$, the sufficient conditions are $\bar{\Delta} > 0$, 2d < b and $2qS^* \leq 1$, where

$$\bar{\Delta} = b^2 (1 - 2qS^*)^2 + 8(\alpha + d)(bqS^* - b + d), \ \tau_t = \frac{b(1 - 2qS^*) + \sqrt{\bar{\Delta}}}{4(b - d - bqS^*)}, \ \tau_b = \frac{b(1 - 2qS^*) - \sqrt{\bar{\Delta}}}{4(b - d - bqS^*)}.$$



148 Page 6 of 28 Q. Liu et al.

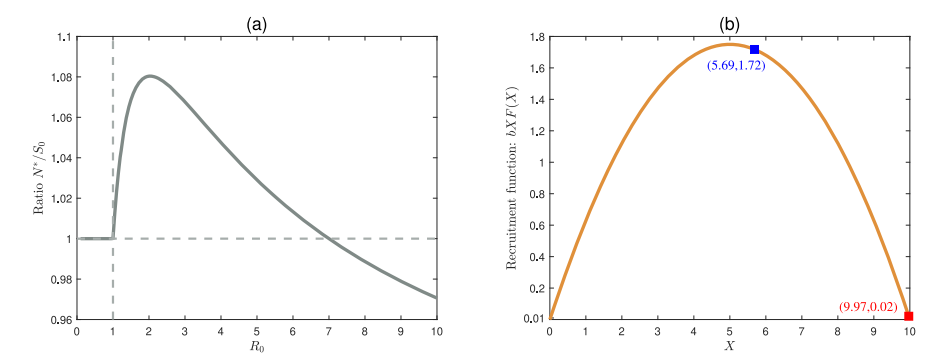


Fig. 1 An illustration of the disease-induced hydra effect due to resource competition in system (1). (a) A disease-induced hydra effect occurs for $1 < R_0 < 7$ (varying β). (b) The recruitment function bXF(X) as population size X changes and with $\beta = 0.6985$ (ratio $N^*/S_0 = 1.0002$) fixed. The blue square indicates the reproducing population size $(S^* + \tau I^* \approx 5.69)$, and the red square represents the total population size $(S^* + I^* \approx 9.97)$ in the epidemiological system (1). Parameter values are b = 0.7, $\tau = 0.5$, q = 0.1, d = 0.00001, r = 0.8, $\alpha = 0.2$. The initial values are $(S_0, I_0) = (170, 2)$ (color figure online)

We note that there is no disease-induced hydra effect in system (1) when $\tau = 1$.

The proof is presented in Appendix C.

The existence of the disease-induced hydra effect in epidemiologic model (1) is due to the overcompensatory nature of resource competition in the recruitment function bXF(X); i.e., $\frac{d}{dX}(bXF(X)) < 0$ for some interval (Jaramillo et al. 2022). The total equilibrium population in the epidemiological system is $S^* + I^*$ (red square), while the total equilibrium in the reproducing population is $S^* + \tau I^*$ (blue square), shown in Fig. 1(b). It can be seen from Fig. 1(b) that by reducing the size of the reproductive population, the concave-down form of the recruitment function bXF(X) allows the population to increase recruitment significantly. The increased recruitment compensates for the population loss caused by disease-induced mortality, allowing the endemic population size ($N^* = S^* + I^*$) to exceed the disease-free population size (S_0). Given Theorem 3, we see that such a disease-induced hydra effect may exist in epidemiological model (1), as determined by the parameter τ .

In the next section, we analyze the co-evolutionary invasion process of host defense and pathogen virulence, and we derive the co-evolutionary dynamics of host–pathogen interaction. We choose our parameters such that the disease persists in the system (i.e., $R_0 > 1$) at an endemic equilibrium (S^*, I^*) .

3 Co-evolutionary dynamics of host-pathogen interactions

The interaction between host and pathogen drives a co-evolutionary process, and the long-term behaviour of their interactions may depend on the interplay of evolutionary traits in both species. Consequently, we assume that host defense will evolve in tandem with the evolving virulence of the pathogen. Since developing host defenses is costly, we hypothesize that increased host defense is associated with a decreased rate of host reproduction b. There are two alternative types of defense: resistance (R) and tolerance



(T) (Boots et al. 2009). We consider a combined strategy using these two types of defense to reduce both the disease-induced mortality α and the transmission rate β . We model host investment in the immune system as a combined host-defense strategy, represented by a single phenotypic trait x. Pathogen virulence is represented by a single phenotypic trait y, and we assume that the transmission rate β and disease-induced mortality α are positively related to y. Note that y is a genetic trait of the pathogen only. Furthermore, host investment x and pathogen virulence y have a physiological maximum, which we denote by x_{max} and y_{max} , respectively. The feasible trait region is denoted by $\mathbb{C} = [0, x_{max}] \times [0, y_{max}]$. Thus, system (1) becomes

$$\frac{dS}{dt} = b(x)(S + \tau I)(1 - q(S + \tau I)) - \beta(x, y)SI - dS + \gamma I,$$

$$\frac{dI}{dt} = \beta(x, y)SI - (\alpha(x, y) + d + \gamma)I.$$
(2)

Physiological considerations suggest that the arbitrary forms of the trade-off functions b(x), $\alpha(x, y)$ and $\beta(x, y)$ have the following properties with $x, y \in \mathbb{C}$:

- (H1) b(x) is a positive function and b'(x) < 0;
- (H2) $\alpha(x, y)$ is a non-negative function, $\alpha'_x(x, y) < 0$ and $\alpha'_y(x, y) > 0$;
- (H3) $\beta(x, y)$ is a non-negative function, $\beta'_x(x, y) < 0$ and $\beta'_y(x, y) > 0$.

In this context, evolution is modelled as a sequence of steps of trait invasion and substitution under the assumptions of finitely small and rare mutational events and clonal reproduction (Vitale and Best 2019). Denote the resident traits as (x, y) and the mutant traits as (x_m, y_m) . Based Baalen's method (Baalen 1998), we use the expected lifetime reproductive success of an individual as the invasion fitness for the mutant host (see Appendix D for details). We obtain

$$f_1(x_m, x, y) = \frac{b(x_m)(d + \alpha(x_m, y) + \gamma + \beta(x_m, y)I^*(x, y)\tau)F(S^*(x, y) + \tau I^*(x, y))}{(d + \beta(x_m, y)I^*(x, y))(d + \alpha(x_m, y) + \gamma) - \beta(x_m, y)I^*(x, y)\gamma}.$$

If $f_1(x_m, x, y) > 1$, the mutant host will increase, and we claim that the mutant host can invade when the resident is at equilibrium. Note that $f_1(x_m, x, y) \mid_{x_m = x} = f_1(x, x, y) = f_1(x, y) = 1$.

Further, we use the basic reproduction number of a rare mutant as the invasion fitness for mutant pathogen (see Appendix D), which is given by

$$f_2(y_m, x, y) = \frac{\beta(x, y_m)S^*(x, y)}{d + \alpha(x, y_m) + \gamma}.$$

If $f_2(y_m, x, y) > 1$, the population density of the mutant pathogen can invade. Note that $f_2(y_m, x, y) |_{y_m = y} = f_2(y, x, y) = f_2(x, y) = 1$. Furthermore, in line with most evolutionary modelling studies, we assume that invasion implies trait substitution; namely, the resident is — after a period of epidemic transmission that is short at the timescale of mutation — monomorphic again, but with a different trait (Geritz et al. 2002).



148 Page 8 of 28 Q. Liu et al.

Through successive invasion and replacement, the host defense and pathogen virulence will evolve step by step. The evolutionary direction is determined by the signs of selection gradients $g_1(x, y)$ and $g_2(x, y)$, which are

$$g_{1}(x, y) = \frac{\partial f_{1}(x_{m}, x, y)}{\partial x_{m}} \bigg|_{x_{m} = x}$$

$$= \frac{F(S^{*}(x, y) + \tau I^{*}(x, y)) * G(x, y)}{((d + \beta(x, y)I^{*}(x, y))(d + \alpha(x, y) + \gamma) - \beta(x, y)I^{*}(x, y)\gamma)^{2}},$$

$$g_{2}(x, y) = \frac{\partial f_{2}(y_{m}, x, y)}{\partial y_{m}} \bigg|_{y_{m} = y}$$

$$= \frac{S^{*}(x, y)(\beta'_{y}(x, y)(d + \alpha(x, y) + \gamma) - \beta(x, y)\alpha'_{y}(x, y))}{(d + \alpha(x, y) + \gamma)^{2}},$$

where

$$\begin{split} G(x,y) &= (b'(x)(d+\alpha(x,y)+\gamma+\beta(x,y)I^*(x,y)\tau) + b(x)(\alpha_X'(x,y)+\beta_X'(x,y)I^*(x,y)\tau)) \\ &\times ((d+\beta(x,y)I^*(x,y))(d+\alpha(x,y)+\gamma) - \beta(x,y)I^*(x,y)\gamma) - b(x)(d+\alpha(x,y)+\gamma+\beta(x,y)I^*(x,y)\tau) + (d+\beta(x,y)I^*(x,y)\alpha_X'(x,y)I^*(x,y)(d+\alpha(x,y)) \\ &+ (d+\beta(x,y)I^*(x,y)\alpha_X'(x,y)). \end{split}$$

Rapid rates of sequence change are typically observed when viral evolution is measured on short timescales; however, on longer timescales, pathogens evolve several orders of magnitude slower, approaching those of their hosts (Simmonds et al. 2019; Aiewsakun and Katzourakis 2016). Since the mutant is small and rare, at the slow time-scale of evolution T we can approximate the expected value of phenotypic traits (x, y) as (Yang et al. 2022; Vitale and Best 2019)

$$\frac{dx}{dT} \approx \mu_x g_1(x, y),
\frac{dy}{dT} \approx \mu_y g_2(x, y),$$
(3)

where μ_x and μ_y are positive coefficients that take into account the evolutionary speed and variance of the mutation process. An evolutionary singular strategy (x^*, y^*) satisfies $g_1(x, y) = 0$ and $g_2(x, y) = 0$ (Cressman 2010; Christiansen 1991). In particular, when $\mu_x = 0$ (resp. $\mu_y = 0$), only the evolution of virulence (resp. host defense) is considered; i.e., a mono-trait evolution case. We assume that superinfection does not occur. We link within-host dynamics (3) to between-host dynamics (1) through co-evolution of pathogen virulence and host defense.

3.1 Continuously stable strategy

Next, we study the convergence stability (CS) and evolutionary stability (ES) of the evolutionary singular strategy (x^*, y^*) . We use the linear approximation method (Yang



et al. 2022) to estimate the convergence stability of the evolutionary singular strategy in system (3). The Jacobian matrix J at the singular strategy (x^*, y^*) is given by

$$J(x^*, y^*) = \begin{bmatrix} \mu_x \frac{\partial g_1(x, y)}{\partial x} & \mu_x \frac{\partial g_1(x, y)}{\partial y} \\ \mu_y \frac{\partial g_2(x, y)}{\partial x} & \mu_y \frac{\partial g_2(x, y)}{\partial y} \end{bmatrix} \Big|_{\substack{x = x^* \\ y = y^*}}.$$
 (4)

The evolutionary singular strategy (x^*, y^*) is locally convergence stable provided that

$$\det[J(x^*, y^*)] = \mu_x \mu_y \left(\frac{\partial g_1(x, y)}{\partial x} \frac{\partial g_2(x, y)}{\partial y} - \frac{\partial g_1(x, y)}{\partial y} \frac{\partial g_2(x, y)}{\partial x} \right) \Big|_{\substack{x = x^* \\ y = y^*}} > 0,$$

$$\operatorname{tr}[J(x^*, y^*)] = \left(\mu_x \frac{\partial g_1(x, y)}{\partial x} + \mu_y \frac{\partial g_2(x, y)}{\partial y} \right) \Big|_{\substack{x = x^* \\ y = y^*}} < 0$$

hold true; i.e., a population with a nearby strategy can be invaded by a mutant that is even closer to (x^*, y^*) (Smith 1982).

If the evolutionary singular strategy (x^*, y^*) cannot be invaded by any nearby strategy, this indicates that it is evolutionarily stable (Smith 1982). One can estimate this by calculating the second-order derivatives of the host and pathogen invasion fitness functions with respect to the mutant trait (Yang et al. 2022; Zu et al. 2020) as follows:

$$\frac{\partial^{2} f_{1}(x_{m}, x, y)}{\partial x_{m}^{2}} \bigg|_{\substack{y=y^{*} \\ x_{m}=x=x^{*}}} < 0, \quad \frac{\partial^{2} f_{2}(y_{m}, x, y)}{\partial y_{m}^{2}} \bigg|_{\substack{x=x^{*} \\ y_{m}=y=y^{*}}} < 0.$$
 (5)

An evolutionary singular strategy (x^*, y^*) that is both convergence stable and evolutionarily stable is a continuously stable strategy (CSS) and represents a final endpoint of the evolutionary process (Zu et al. 2011). For the continuously stable strategy (x^*, y^*) , the monomorphic host and monomorphic pathogen can stably coexist on a long-term evolutionary timescale. The co-evolutionary process of traits stops when a continuously stable strategy (CSS) or the extinction boundary of one species is reached (Geritz et al. 1998). When the singularity cannot be achieved — i.e., it is not convergent stable — it is referred to as a repeller.

3.2 Specific Trade-Offs

From Eqs. (4)–(5), we can see that whether the singular strategy (x^*, y^*) is a CSS depends on the curvature of the trade-off function at (x^*, y^*) and the population density $(S^*(x, y), I^*(x, y))$. Under epidemiological considerations, we obtain arbitrary trade-off forms (H1)–(H3) that are biologically meaningful. To give an example to illustrate the case of CSS, we take the following general trade-off function:

$$b(x) = \frac{b_0}{1 + b_1 x}.$$



148 Page 10 of 28 Q. Liu et al.

We choose the simple form of the birth rate b(x); specifically, we choose the coupled form of transmission rate $\beta(x, y)$ and disease-induced mortality $\alpha(x, y)$:

$$\beta(x, y) = \frac{\beta_0}{1 + \beta_1 e^{(\beta_2 x - \beta_3 y)}}, \ \ \alpha(x, y) = \frac{\alpha_0 y^n}{1 + \alpha_1 x^n + \alpha_2 y^n},$$

where β_0 is the maximum transmission rate, β_1 adjusts the concavity and convexity, and β_2 and β_3 are the shape parameters of the function that characterizes the asymmetric interaction. Note that $\beta(x, y)$ is a sigmoidal function if $\beta_2 = \beta_3$, which approaches a step function as β_2 or β_3 increases. This function can be suitable for a variety of asymmetric interactions (Mougi and Iwasa 2010; Yang et al. 2022; Nuismer et al. 2007; Kisdi 1999). It takes a flexible form that is more consistent with empirical evidence and is applicable to a wider range of asymmetric host–pathogen interactions (Yang et al. 2022). The function $\alpha(x, y)$ is a monotonically decreasing (resp. increasing) function with respect to x (resp. y), where α_0 is the maximum mortality rate, α_1 weighs the negative effect of host defense on the mortality rate and α_2 is the parameter that measures the saturation effect of virulence. Finally, n is the shape parameter. All parameters are non-negative.

Note that we consider combined-host strategies; that is, host defense refers to both resistance and tolerance. When $\beta_2 = 0$ (resp. $\alpha_1 = 0$), host defense refers only to tolerance (resp. resistance), a pure strategy. An example illustrating a CSS for host–pathogen co-evolution is given in Fig. 2. It can be seen from Fig. 2(c)–(d) that natural selection keeps hosts and pathogens evolving towards the maximal fitness level.

4 Numerical simulations

In the following, numerical simulations are carried out to illustrate how co-evolutionary adaptation affects the dynamic behavior of the population sizes and trait values by changing some parameters of interest.

4.1 Evolutionary cycling

From Theorem 2, it follows that there are no periodic orbits in system (1) at $\tau=0$. This means that if the infection completely inhibits recruitment, the number of infected individuals can be controlled at a stable state, without bifurcations or extreme fluctuations. However, epidemiological feedback on host–pathogen co-evolution may yield long-term periodic oscillations in traits (Yang et al. 2022; Ashby and Boots 2015) and consequently in the host equilibrium density, as shown in Fig. 3. The local asymptotic stability of the evolutionary singularity strategy (x^*, y^*) implies convergence stability. Mathematically, if the strategy (x^*, y^*) is not convergence stable, then model (3) may exhibit a Hopf bifurcation; that is, the phenotypic traits may evolve to a stable limit cycle (see Fig. 3(a)). This suggests that host–pathogen co-evolution may complicate disease propagation and play a crucial role in disease-transmission patterns.

Further, we examine how the reduction factor τ influences evolutionary cycling within the remaining parameter range ($\tau \in (0, 1]$). As shown in Fig. 4(a), evolutionary



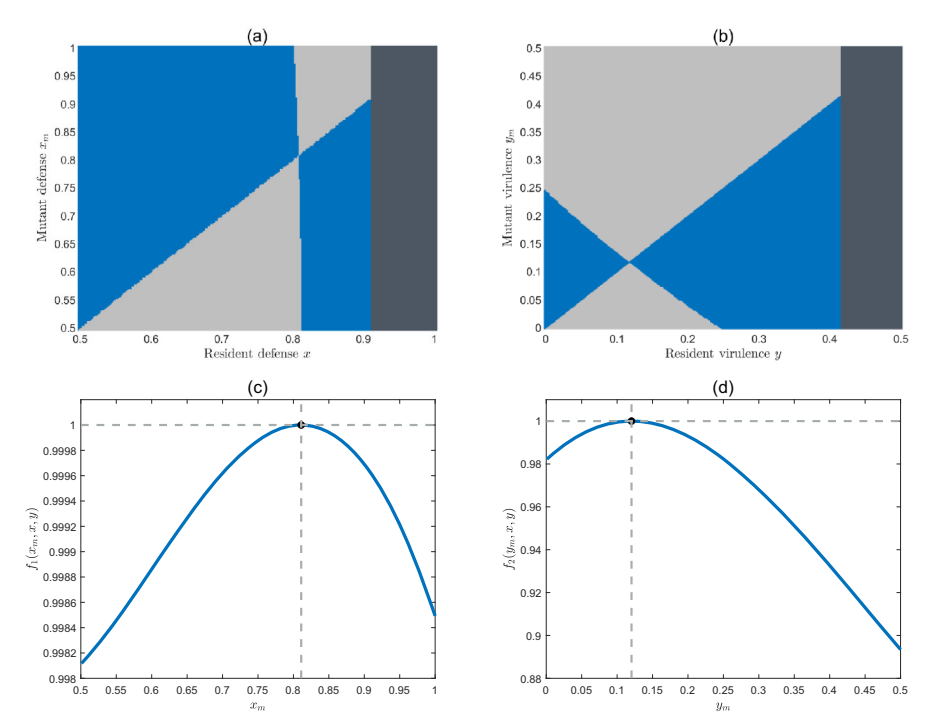


Fig. 2 Continuously stable strategy of host–pathogen co-evolution. Pairwise invasibility plots (PIP) for (a) fixed-pathogen-virulence strategy $y=y^*=0.12$ and (b) fixed-host-defense strategy $x=x^*=0.81$. The blue regions indicate the feasible invasion regions of the invading traits (mutant host defense (a) and mutant virulence (b)). The dark grey region marks the disease-extinction space. Invasion fitness landscape of the mutant defense (c) and of the mutant virulence (d) when the resident strategy is $(x,y)=(x^*,y^*)$. Parameter values are $b_0=0.8$, $b_1=0.25$, $\tau=0.5$, q=0.15, d=0.005, $\alpha_0=0.5$, $\alpha_1=0.5$, $\alpha_2=1$, $\beta_0=0.2$, $\beta_1=1.5$, $\beta_2=1$, $\beta_3=0.4$, $\gamma=0.28$, $\mu_x=0.01$, $\mu_y=0.1$ and n=2, with initial condition $(x_0,y_0)=(0.4,0.6)$ (color figure online)

cycling does not occur when the reduction τ is relatively small, but it emerges when τ is increased, resulting in the associated population cycling (see Fig. 4(b)). This indicates that the lower the degree of recruitment inhibition by infection, the more likely evolutionary cycling is to occur. Note that the amplitude of oscillations in the trait value of the pathogen (y) is much larger than that of the host (x) as the host and pathogen co-evolve, as shown in Fig. 4(a). This difference can be explained by considering variations in the sensitivity of trait dynamics to epidemiological feedback between species (Mougi and Iwasa 2010). From an epidemiologic perspective, this difference, in turn, leads to greater oscillations in the population size of the infected than in that of susceptibles over the long term (see Fig. 4(b)). The amplitudes of infected individuals fluctuate the most at an intermediate level of reduction τ (around $\tau = 0.6$), whereas the amplitudes of susceptibles and traits are relatively insensitive to variations in τ . This means that, under the influence of co-evolution, if the infection partially inhibits recruitment, the result may be a wider range of disease fluctuations, compared to the case of completely unaffected recruitment.



148 Page 12 of 28 Q. Liu et al.

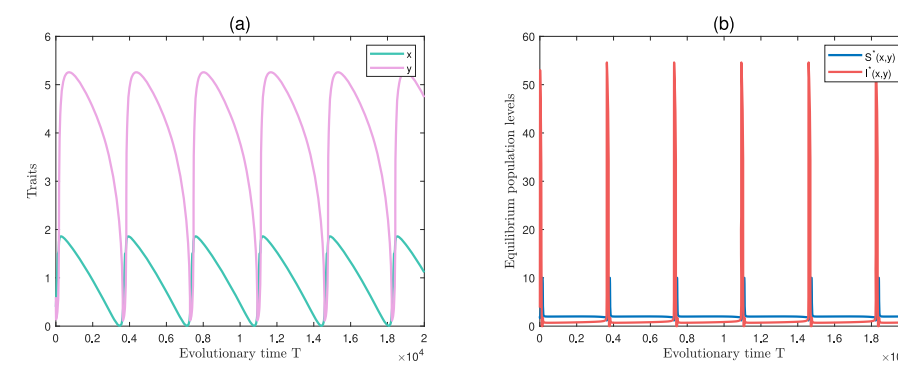


Fig. 3 Evolutionary cycling for $\tau=0$. (a) Time series curves of traits x(t) and y(t) obtained though simulation model (3) with initial condition $(x_0, y_0)=(0.4, 0.6)$. (b) Corresponding evolving equilibrium population level of the host (both the susceptible $S^*(x, y)$ and infectious $I^*(x, y)$) when the traits x and y co-evolve. Parameter values are $b_0=0.8$, $b_1=0.2$, q=0.1, d=0.00005, $\alpha_0=1.2$, $\alpha_1=0.5$, $\alpha_2=0.8$, $\beta_0=0.8$, $\beta_1=2.5$, $\beta_2=2$, $\beta_3=1.55$, $\gamma=0.2$, $\mu_x=0.005$, $\mu_y=0.1$ and n=2

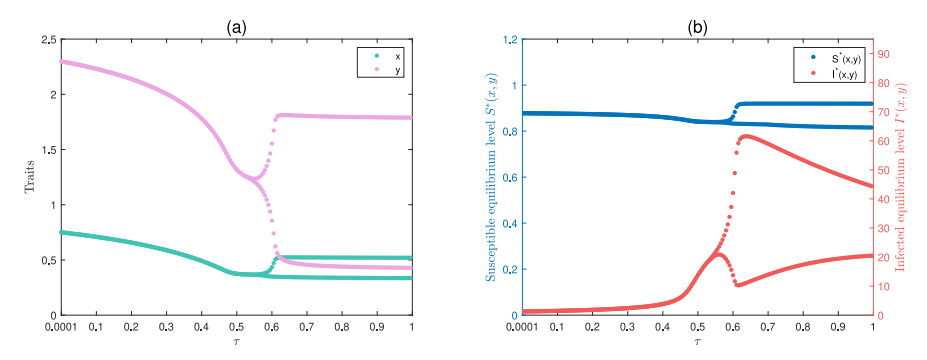


Fig. 4 Bifurcation diagrams of trait dynamics (a) and corresponding population equilibrium level (b) in relation to the reduction τ . The points indicate the minimum and maximum values. Parameter values are q = 0.02, $\alpha_0 = 0.5$, $\beta_1 = 2$, $\beta_2 = 1.85$, $\beta_3 = 2$ and $\gamma = 0.17$. Remaining parameters are as in Fig. 3

It should be mentioned that in epidemiological model (1), which does not incorporate evolutionary adaptation, numerical simulations show that there is no periodic solution for $\tau \in (0, 1]$ under the parameters of Fig. 4. Due to the complex nonlinearity, the result of evolutionary cycling is only illustrated by numerical simulation examples. Next, we focus on CSS strategies (x^*, y^*) to study stable investments in host–pathogen interaction mechanisms.

4.2 Evolution-driven disease-prevalence patterns

To investigate the role of co-evolution in driving host defense and pathogen virulence selection, we examine its feedback on disease prevalence P under different ecological conditions. We have $P = I^*(x^*, y^*)/(S^*(x^*, y^*) + I^*(x^*, y^*))$, where $S^*(x^*, y^*)$ and $I^*(x^*, y^*)$ denote the susceptible and infected host equilibrium levels at CSS strategies (Singh and Best 2023). We first consider the situation as the recovery rate



 γ changes, where an increase in recovery may be attributed to the effects of improved environmental hygiene, such as improved living conditions enhancing the host's physiological state. It follows from Fig. 5(a) that the prevalence is a decreasing function of γ in the absence of host evolution (only pathogen evolution P_v or no evolution P_o), but an increasing function of γ when hosts co-evolve (P_{co}). This implies that co-evolution could reverse the disease-prevalence pattern corresponding to the recovery rate γ .

For non-evolving strategies (traits x and y are constants), increased recovery rates simply indicate that fewer hosts remain in the infected state, thus lowering the disease prevalence P_o ; i.e., P_o decreases as γ increases. When considering pathogen evolution only, the pathogen evolves gradually towards higher virulence levels with increasing recovery rate γ ; i.e., CSS y_n^* is an increasing function in γ (Fig. 5(b)). Increased virulence yields an elevation in transmissibility; however, the resulting higher infectivity is insufficient to compensate for the shorter duration of infection caused by improved recovery and disease-induced mortality. Thus the prevalence P_v , despite being maintained at a higher level, decreases continuously with increasing γ , consistent with the no-evolution scenario. When the host co-evolves, we see that both host defense and pathogen virulence evolve towards lower levels with increasing recovery, but virulence is maintained at a higher level than the pathogen mono-evolution case. This implies that host co-evolution could shift the direction of pathogen evolution and cause an increase in overall virulence levels. Hence, this co-evolution allows increases in transmissibility and mitigations in disease-related mortality to outweigh increases in recovery, resulting in an overall increase in prevalence, thereby reversing the disease pattern corresponding to recovery rates.

When evolution is not considered, an increase in the recovery rate accelerates the transition of individuals from the infected class (I) back to the susceptible class (S), while also decreasing R_0 . The reduction in R_0 indicates that the number of secondary cases generated by an infected individual during their infectious period in a fully susceptible population decreases, meaning the inflow of infected individuals is reduced. Consequently, the steady-state proportion of infected individuals in the population also gradually decreases. Therefore, disease prevalence should be a decreasing function of the recovery rate. However, when co-evolution is considered, disease prevalence increases with the recovery rate. This means that as the recovery rate increases, the steady-state proportion of infected individuals in the population paradoxically increases. Fig. 5 illustrates this phenomenon, where the gray dashed line decreases as the recovery rate γ increases.

The counter-intuitive phenomenon of prevalence reversal means that any medication designed to improve recovery without affecting pathogen transmission and toxicity may result in potentially higher disease prevalence due to host-pathogen interaction. This is consistent with the conclusions in Gandon et al. (2003, 2001), but we additionally emphasize the role of host co-evolution in our study. Our results further suggest that host evolution could induce selection for highly virulent pathogens $(y_{co}^* > y_v^*)$ in Fig. 5(b)), indicating that any imposed changes in host-defense medication may risk selection for high virulence. Pathogen evolution is highly sensitive to that of the host (Best et al. 2009), which could result in the evolution of highly virulent pathogens (Buckingham and Ashby 2022). There is evidence that the high immune adaptability of some variants to their host could further enhance infection



148 Page 14 of 28 Q. Liu et al.

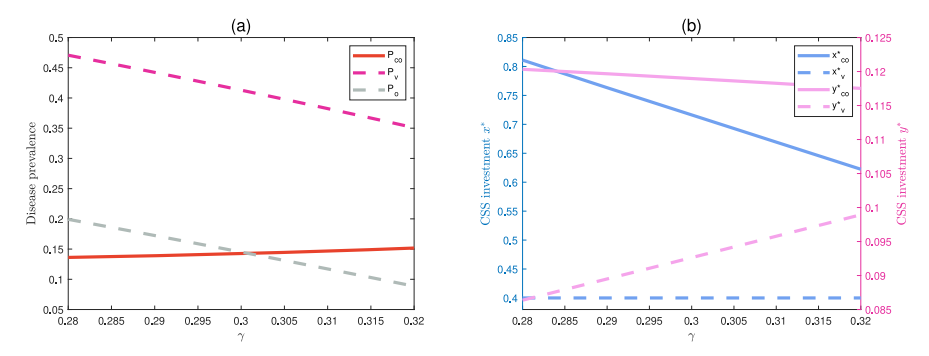


Fig. 5 An illustration of prevalence reversal resulting from co-evolution. (a) Patterns displaying how evolution drives the disease prevalence P for varying γ with host co-evolution (P_{co}), without host co-evolution (P_v , $\mu_x = 0$) and without evolution (P_v , $\mu_x = \mu_y = 0$). (b) CSS investment variation in (x^* , y^*) as γ varies with and without host co-evolution. Parameters are as in Fig. 2

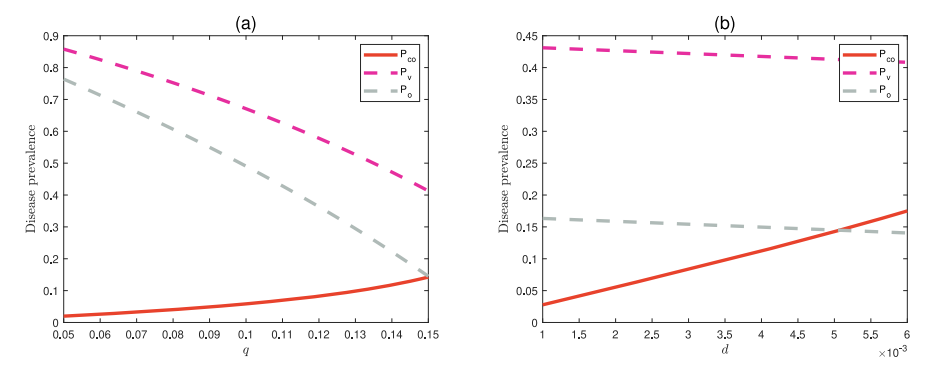


Fig. 6 An illustration of prevalence reversal resulting from co-evolution for a varying environment. The environment was changed by varying (a) the crowding effect q (when d=0.005) and (b) the natural mortality rate d (when q=0.15) with $\gamma=0.3$ fixed. Remaining parameters are as in Fig. 2

(McCallum et al. 2022; Day et al. 2022). Our focus is illustrating that host evolution could also exert a strong impact on pathogen evolution, yielding unexpected epidemiological scenarios. In Section 4.3, we use numerical simulations to demonstrate two different transmission patterns, which further illustrates the necessity for considering this co-evolutionary effect rather than a separate evolutionary effect.

We further examine the case of changing the environment (via varying crowding effect q and natural mortality rate d). Fig. 6 shows that co-evolution could reverse the patterns of disease prevalence corresponding to q and d, yielding similar conclusions as above. This suggests that prevalence reversal may not be an uncommon scenario in the context of host–pathogen co-evolution. In addition, from Figs. 5 and 6, we found that considering only the evolution of pathogens may overestimate disease prevalence (P_v is above P_{co} and P_o). The decline in prevalence is greater under no evolution in all cases, as shown in Fig. 6. The above results suggest that host–pathogen co-evolution is closely linked to disease prevalence and that for a better understanding, we need to take into account this co-evolutionary effect rather than a separate evolutionary one.



4.3 Two different transmission patterns resulting from co-evolution

We assume that both the transmission rate $\beta(x, y)$ and the disease-induced mortality rate $\alpha(x, y)$ are binary functions of host defense x and pathogen virulence y. Over time, host defense and pathogen virulence co-evolve until the evolutionary process reaches an endpoint (CSS strategy (x^*, y^*)); consequently, $\beta(x, y)$ and $\alpha(x, y)$ vary until stabilization is achieved. The transmission and disease-induced mortality rate will remain constant for a long time until the external environment changes and restabilizes again. Next, we consider the general scenario where the recovery rate γ varies and obtain an illustration of the two transmission patterns in Fig. 7.

From Fig. 7(a), we found that the steady-state disease-induced mortality rate $\alpha(x^*, y^*)$ initially increases with increasing recovery γ (for $\gamma < \gamma^{\alpha}$) but begins to decline as γ continues rising, forming a concave-down shape. The steady-state transmission rate $\beta(x^*, y^*)$ increases with recovery, and its gradient remains positive but becomes less steep at higher recovery rates. This suggests that altering recovery may sequentially cause two different transmission patterns, resulting in a reversal of the prevalence (see P_{co} in Fig. 7(b)). The biological interpretation for this difference can be given by the following intuitive explanation.

Initially, the pathogen evolves to compensate for losses due to more rapid removals by increasing virulence y^* as recovery increases. Since the virulence is not too high and the infected host lives long enough to infect new susceptible individuals, pathogens could benefit. However, with further increments in recovery and virulence, the infected groups decrease rapidly, and the pathogen is unable to compensate for the decline in infected hosts through higher virulence, making increased virulence an inappropriate strategy. Hence, increasing virulence is not sufficient to maintain fitness at high recovery ($\gamma > \gamma^y$), and the pathogen would evolve towards lower virulence to reduce additional mortality instead. Since hosts can contribute to fitness once they return to the susceptible state, increasing recovery leads to less selection for host defense. Consequently, with increasing recovery, CSS virulence y^* is a concave-down shape, but host defense x^* is monotonically decreasing (Fig. 7(b)). The predominance of low virulence and defense results in higher transmission but lower mortality within the population, leading to prevalence reversal.

The first transmission pattern is both highly infectious and lethal, such as the plague (Pechous et al. 2016), but is seldom observed. For most emerging pathogens (that have just crossed species to a new host, such as humans), there is often no history of long-term co-evolution with the new host. As a result, those pathogens tend to exhibit relatively high virulence, due to uncontrolled replication and severe tissue damage in the host, as well as high transmissibility, because of a large amount of replication and a high amount of virus excretion (Bonneaud and Longdon 2020). However, in the long term, pathogens that maintain both high transmission and high lethality are less common (Kun et al. 2023). The second transmission pattern occurs more frequently. This high-infectivity and low-lethality characteristic, as a universal feature of pathogen evolution in the long term, is highly conducive to pathogen spread, as observed in the common cold. Our co-evolutionary framework simulates these two successive modes of transmission, which, to the best of our knowledge, are not available in related



148 Page 16 of 28 Q. Liu et al.

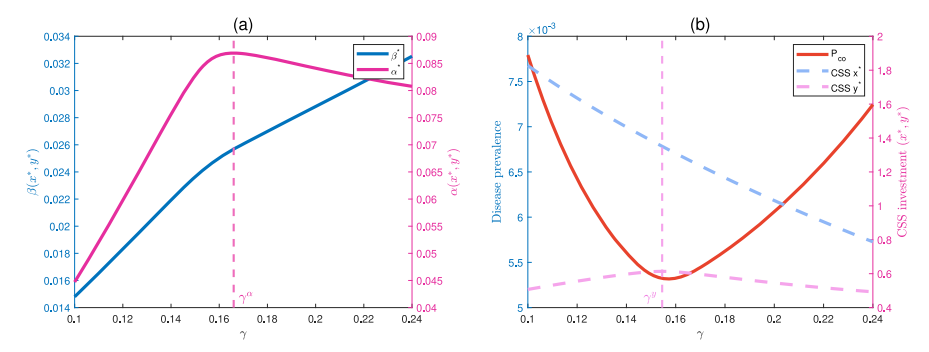


Fig. 7 An illustration of how co-evolution induces two transmission patterns for varying recovery rate γ . (a) Transmission rate $\beta(x^*, y^*)$ and disease-induced mortality $\alpha(x^*, y^*)$ at corresponding CSS strategies (x^*, y^*) for varying γ . (b) CSS investment variation in (x^*, y^*) and corresponding disease prevalence P_{co} along with varying γ . The vertical dashed lines indicate two thresholds $\gamma^{\alpha} = 0.166$ and $\gamma^{y} = 0.1545$. Parameter values are $b_1 = 0.3$, q = 0.1, d = 0.002, $\alpha_2 = 0.8$, $\beta_0 = 0.1$, $\beta_1 = 1.8$ and $\beta_3 = 1.31$. Remaining parameters are as in Fig. 2

mathematical-modelling studies. The above analysis shows that host-pathogen coevolution may be responsible for some specific patterns of transmission; as such, we need to take this co-evolution into account.

4.4 Impact of host-pathogen co-evolution on hydra effects

From Theorem 3, we see that a disease-induced hydra effect may arise from resource competition and reduced recruitment ($0 \le \tau < 1$) by infectious individuals. There is a threshold recruitment value of τ for this hydra effect. In the following, we examine the impact of evolution on the disease-induced hydra effect.

In the absence of evolution, host defense x and pathogen virulence y are constants. The ratio of the endemic population size to the disease-free population size is $N^*(x_0, y_0)/S_0(x_0, y_0)$, which we denote as the o-ratio, where (x_0, y_0) are the initial resident traits. From Fig. 8(a), we see that a disease-induced hydra effect could arise in model (2) and that there is no such hydra effect at $\tau = 0$ (pink dot, o-ratio < 1) when $R_0 = 3.4279$ ($\beta_0 = 0.8$). We then illustrate in Fig. 8(b)–(c) (grey dashed curve, right axis) the reduction threshold for the disease-induced hydra effect in the absence of evolution. It shows that o-ratio > 1 only occurs for $0.041 \le \tau \le 0.551$. This means that, without evolution, a disease-induced hydra effect occurs when an infected individual's contribution to recruitment is about 4-55% of a susceptible individual's contribution. With co-evolution, host defense co-evolves with pathogen virulence until it reaches an evolutionary endpoint (CSS strategies). When the disease is eliminated, host defenses decrease to zero, but the pathogen can still evolve further in the environment until virulence stabilizes. Thus, the ratio becomes $N^*(x^*, y^*)/S_0(0, \bar{y}_0)$ when the host and pathogen co-evolve, denoted as co-ratio N^*/S_0 , where (x^*, y^*) are the CSS strategies and \bar{y}_0 is the steady-state pathogen virulence in vitro. It follows from Fig. 8(b) that co-ratio < 1 in the entire range of τ (the blue solid curve is below 1). This implies that host-pathogen co-evolution may induce the vanishing of the disease-induced



hydra effect. Without host evolution, the ratio becomes $N^*(x_0, y_v^*)/S_0(x_0, \bar{y}_0^v)$, which we denote as the v-ratio, where y_v^* and \bar{y}_0^v are the CSS strategies in the presence and absence of disease, respectively. As can be seen in Fig. 8(c), compared to the no-evolution scenario, the range of τ where the hydra effect can occur is wider in the absence of host evolution, approximately $0.001 \le \tau \le 0.961$ (v-ratio > 1). In addition, the corresponding change in ratio amplitude increases. This suggests that considering pathogen evolution alone may overestimate the scope and magnitude of the disease-induced hydra effect.

Comparing Fig. 8(b) with Fig. 8(c), our results illustrate that host–pathogen coevolution may result in the loss of the disease-induced hydra effect, whereas pathogen mono-evolution strengthens said hydra effect (both the existence range and the magnitude). The pattern shown in Fig. 8 is obtained by assuming that, in the no-evolution scenario, model (2) does not have a disease-induced hydra effect at $\tau = 0$, but similar conclusions are reached even if we choose the presence of such hydra at $\tau = 0$, shown in Fig. 9, which we achieved by changing the initial resident traits (x_0, y_0) . In this case, the disease-induced hydra effect occurs at the pink dot when it did not in Fig. 8(a). Our work emphasizes the potential role of host–pathogen interactions in epidemic infections, which could lead to different epidemiological effects. Therefore, taking such co-evolutionary interactions into account is a necessary step towards a better understanding of disease infection.

5 Discussion

Host–pathogen interactions are a typical co-evolutionary process. Establishing a basic framework for such co-evolutionary dynamics is therefore essential for a comprehensive understanding of evolutionary mechanisms and outcomes. We studied the co-evolutionary interactions between host defense and pathogen virulence, which are generally modelled separately. Various forms of defense have been described in natural systems and theoretical models, with two main types of defense available: resistance (*R*) and tolerance (*T*) (Boots et al. 2009). Previously established co-evolutionary models only consider pure defense strategies like tolerance or resistance, whereas in practice, host defense is likely to be a combined strategy (both *R* and *T*). Therefore, based on the theory of adaptive dynamics, we proposed a co-evolutionary model considering a combined host-defense strategy that affects transmission rate and disease-induced mortality, in order to describe the host–pathogen system interactions. The epidemic dynamics are described by an SIS-type model with density-dependent reproduction. Using this modelling framework, the investment levels in defense and virulence, as well as their feedback impact on epidemic transmission, we investigated.

We first analysed the existence and local stability of all possible equilibria for epidemiological system (1) and then examined the global stability of the equilibria at specific τ values. Based on adaptive-dynamics theory, explicit analytic expressions for trait dynamics we derived. We found that the evolutionary outcomes we driven by multiple factors, depending not only on the shape and strength of asymmetric host–pathogen interactions but also on the equilibrium population densities of susceptible and infected hosts. Due to the complex nonlinearity of trait system (3), we



148 Page 18 of 28 Q. Liu et al.

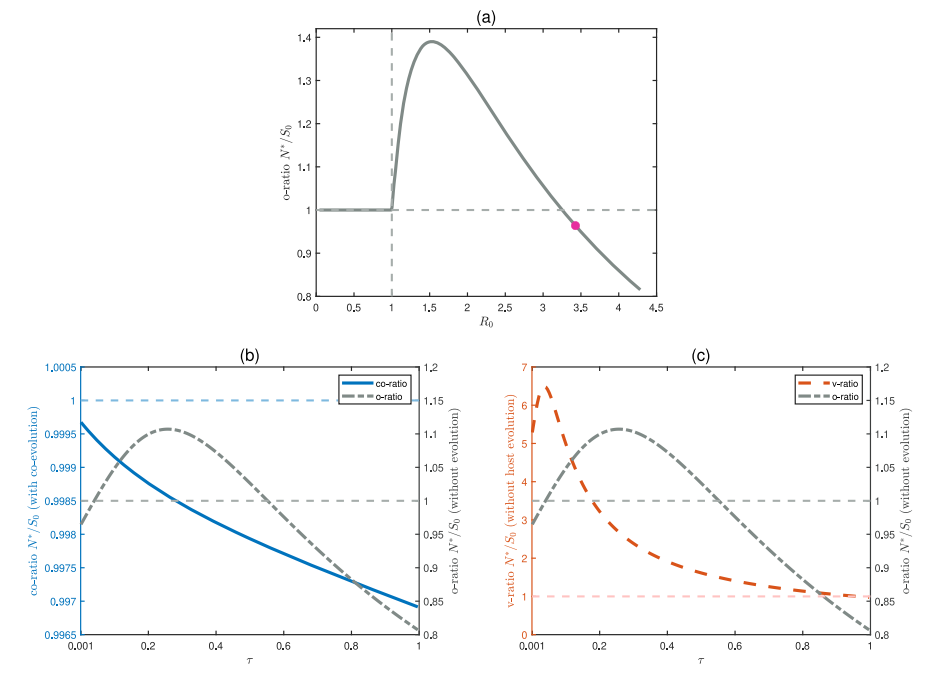


Fig. 8 An illustration of the vanishing of the disease-induced hydra effect due to co-evolution. (a) Without evolution, a disease-induced hydra effect occurs for $1 < R_0 < 3.3$ ($\tau = 0$, varying β_0). The pink dot illustrates the absence of the hydra effect at $\beta_0 = 0.8$. (b) For varying τ , host–pathogen co-evolution causes the disappearance of the disease-induced hydra effect (blue solid curve co-ratio $N^*/S_0 < 1$, left axis). (c) For varying τ , a disease-induced hydra effect occurs for $0.001 \le \tau \le 0.961$ without host evolution (red dashed curve v-ratio, left axis). Without evolution and with $R_0 = 3.4279$ ($\beta_0 = 0.8$) fixed, the disease-induced hydra effect only occurs for $0.041 \le \tau \le 0.551$ (grey dotted curve in (b)–(c), right axis). Remaining parameters are $b_0 = 0.2$, $b_1 = 0.4$, q = 0.2, d = 0.0005, $\alpha_0 = 0.4$, $\alpha_1 = 0.5$, $\alpha_2 = 0.8$, $\beta_0 = 0.8$, $\beta_1 = 1.5$, $\beta_2 = 1$, $\beta_3 = 0.4$, $\gamma = 0.3$ and n = 2. The resident traits are $(x_0, y_0) = (0.6, 0.4)$, with initial condition $(S_0, I_0) = (170, 2)$ (color figure online)

numerically observed evolutionary cycling resulting from host—pathogen co-evolution, which yielded long-term periodic oscillations in infection, even though no cycling was inherent in the corresponding epidemiological system. Further numerical simulations showed that evolutionary cycling was more likely when the recruitment of infection was less inhibited. For variations in the recovery rate, we find that co-evolution may reverse disease-prevalence patterns, compared to no-evolution or pathogen-only-evolution scenarios. Notably, with increasing recovery rate, we observe an illustration of two transmission patterns, whereby the disease is first highly infectious and lethal, then highly infectious but with low lethality. We theoretically demonstrated that a disease-induced hydra effect may exist in epidemiological system (1). Numerical simulations, however, further revealed that host—pathogen co-evolution may lead to the vanishing of the disease-induced hydra effect, whereas pathogen virulence monoevolution strengthens such hydra effect in both range and magnitude. To the best of our knowledge, there are no detailed studies on the two specific transmission modes or the vanishing of the disease-induced hydra effect due to host—pathogen co-evolution.



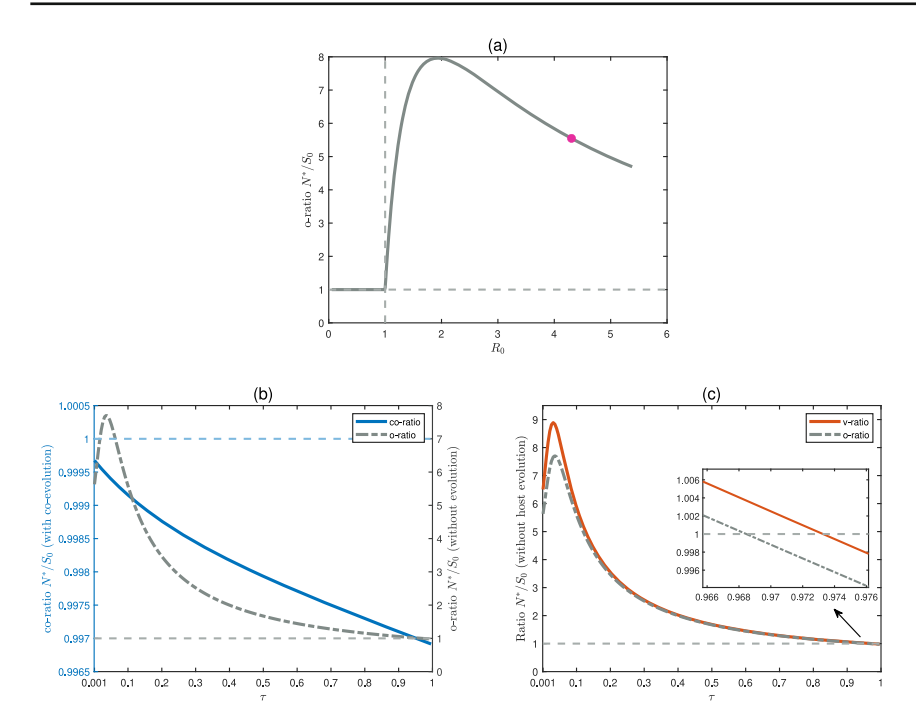


Fig. 9 An illustration of the vanishing of the disease-induced hydra effect due to co-evolution. (a) Without evolution, a disease-induced hydra effect occurs for $R_0 > 1$ ($\tau = 0$, varying β_0). The pink dot illustrates the presence of the hydra effect at $\beta_0 = 0.8$. (b) For varying τ , host-pathogen co-evolution causes the disappearance of the disease-induced hydra effect (blue solid curve co-ratio $N^*/S_0 < 1$, left axis). (c) For varying τ , a disease-induced hydra effect occurs for $0.001 \le \tau \le 0.971$ without host evolution (red dashed curve v-ratio, left axis). Without evolution and with $R_0 = 4.3053$ ($\beta_0 = 0.8$) fixed, the disease-induced hydra effect only occurs for $0.001 \le \tau \le 0.966$ (grey dotted curve in (b)–(c), right axis). Remaining parameters are as in Fig. 8. The resident traits are $(x_0, y_0) = (0.35, 0.12)$, with initial condition $(S_0, I_0) = (170, 2)$ (color figure online)

We focused on combined host-defense strategies, where resistance (R) and tolerance (T) co-evolve simultaneously with pathogen virulence. However, we did not address the question of whether there could be a combined continuously stable strategy (CSS). That is, it may be possible to have no CSS with simultaneous investments to resistance and tolerance, but only pure strategies (only CSS with R or T) when the host favours pure strategies instead of combined ones. To do this, we need to establish host-defense fitness functions for resistance and tolerance (see Appendix E for details) and investigate the issue further in a host-pathogen co-evolutionary context. We leave these for future work. Evolutionary branching, where a continuous trait may converge to a singularity followed by spontaneous splitting of a unimodal trait distribution into a bimodal – or multimodal – one (Wakano and Iwasa 2013), has been a focus of adaptive dynamics research. However, research on evolutionary branching is scarce in the context of host-pathogen co-evolution, and we did not investigate it in this paper but will addressed it in a future study.



148 Page 20 of 28 Q. Liu et al.

Our model has several limitations, which should be acknowledged. We ignored the difference between the reduction in reproduction and resource competition for infectious individuals in our model; future work could consider this difference, the $\tau_1 \neq \tau_2$ case. The evolutionary speeds we constant in our model, whereas organismal mutation rates may vary according to the environment (Duffy et al. 2008). If the evolutionary speeds are considered variables, the situation is much more complicated. We confined the host-defense mechanism to avoidance, but such defense mechanisms are diverse. Therefore, exploring the co-evolution of host and pathogen under different defense mechanisms in conjunction with actual data will be a matter of further research.

We focused on feedback of host—pathogen micro-co-evolutionary effects on macro-epidemics and vice versa, which generated complex biological scenarios. The main results obtained in this work indicate that theory could provide novel insights for future empirical investigations and disease management, given the limited empirical studies on the co-evolution of host and pathogen. We encourage the need for empirical datasets that explicitly measure recovery rates, especially for highly infectious diseases. Specifically, the design of medications on host defense and recovery should be cautious. Further, our work emphasizes that the reduction τ in reproduction and resource competition for infectious individuals may have important implications for disease management, since different levels of reduction may contribute to population cycling and disease-induced hydra effects. This suggests that — for sustained interventions such as improved sanitation or continuous medical interventions that influence the reduction τ or the recovery γ — decision-makers may need to carefully consider the proportion of the infected people who receive such interventions.

Appendix A. Existence and local stability of the ecological equilibria

By calculating the spectral radius of the next-generation matrix for model (1), the basic reproduction number is

$$R_0 = \frac{\beta(b-d)}{bq(\alpha+d+\gamma)}.$$

By direct calculation, we obtain that the boundary equilibrium $E_{00}=(0,0)$ and disease-free equilibrium $E_0=(\frac{b-d}{bq},0)$ always exists for model (1) for b>d. When $R_0>1$, there is a unique positive equilibrium $E=(S^*,I^*)$ for model (1), where

$$S^* = \frac{\alpha + d + \gamma}{\beta}, \quad I^* = \begin{cases} \frac{(\alpha + d + \gamma)(b(\beta - q(\alpha + d + \gamma)) - \beta d)}{\beta^2(\alpha + d)}, & \tau = 0\\ \frac{b\tau(1 - 2qS^*) - \alpha - d + \sqrt{\triangle}}{2b\tau^2q}, & \tau \in (0, 1], \end{cases}$$
$$\triangle = (b\tau(1 - 2qS^*) - \alpha - d)^2 + 4b\tau^2q(bS^*(1 - qS^*) - dS^*).$$

The stability of these equilibria is obtained by analyzing the Jacobian matrix of system (1).

$$J(S,I) = \begin{pmatrix} b(1-2q(S+\tau I)) - \beta I - d \ b\tau(1-2q(S+\tau I)) - \beta S + \gamma \\ \beta I & \beta S - \alpha - d - \gamma \end{pmatrix}.$$



By simple calculation, the Jacobian matrix at E_{00} has two real eigenvalues: (b-d)>0 and $-(\alpha+d+\gamma)<0$. This implies that E_{00} is always an unstable saddle. Similarly, the Jacobian matrix at E_0 has two real eigenvalues: $-\frac{b-d}{b}<0$ and $\frac{\beta(b-d)}{bq}-(\alpha+d+\gamma)$. It is easy to verify that E_0 is locally asymptotically stable when $R_0<1$ and unstable when $R_0>1$. If $R_0>1$, the Jacobian matrix at epidemic equilibrium E^* has a positive determinant $(\det[J(S^*,I^*)]>0)$ and a negative trace $(\operatorname{tr}[J(S^*,I^*)]<0)$, where

$$\det[J(S^*, I^*)] = -\beta I^* (b\tau (1 - 2q(S^* + \tau I^*)) - \beta S^* + \gamma),$$

$$\operatorname{tr}[J(S^*, I^*)] = b(1 - 2q(S^* + \tau I^*)) - \beta I^* - d.$$

Hence, the real parts of its eigenvalues are negative. Thus, E^* is the unique stable equilibrium of the system when $R_0 > 1$ holds.

Appendix B. Global stability of the ecological equilibria at specific au values

To show the global stability of system (1) at $\tau = 0$, denote the right-hand side of the S and I equations in system (1) by \mathcal{P} and \mathcal{Q} , respectively. Taking the Dulac function as $\mathcal{B}(S, I) = \frac{1}{SI}$, we obtain

$$\frac{\partial (\mathcal{BP})}{\partial S} + \frac{\partial (\mathcal{BQ})}{\partial I} = -\frac{bq}{I} - \frac{\gamma}{S^2} < 0$$

for all S > 0 and I > 0. Applying the Dulac–Bendixson Theorem (Dumortier et al. 2006), we can rule out the existence of periodic orbits and homoclinic loops for system (1). Since E_0 is the only locally asymptotically stable equilibrium when $R_0 < 1$ and E is the only locally asymptotically stable equilibrium when $R_0 > 1$, it follows that E_0 and E are globally asymptotically stable when $R_0 < 1$ and $R_0 > 1$, respectively.

For $\tau = 1$, we have $dN/dt = bNF(N) - dN - \alpha I \le N((b-d) - bqN)$. Direct calculation yields

$$N(t) = \frac{(b-d)e^{(b-d)t + (b-d)c}}{1 + bqe^{(b-d)t + (b-d)c}}.$$

Hence, we obtain $N(t) \le (b-d)/bq$. To show the global stability of E_0 , we consider the following Lyapunov function: V(I) = I(t). The time derivative of V(I) computed along solutions of system (1) is



148 Page 22 of 28 Q. Liu et al.

$$\begin{split} \frac{dV}{dt} &= (\beta S - \alpha - d - \gamma)I \\ &\leq (\alpha + d + \gamma) \left(\frac{\beta (b - d)}{bq(\alpha + d + \gamma)} - 1 \right)I \\ &= (\alpha + d + \gamma)(R_0 - 1)I. \end{split}$$

As all parameters are positive, it follows that $dV/dt \le 0$ for all $I(t) \ge 0$ with dV/dt = 0 only at I(t) = 0 when $R_0 < 1$. Applying LaSalle's Invariant Principle (Dumortier et al. 2006), we have $\lim_{t\to\infty} I(t) = 0$. Hence, E_0 is a global attractor of system (1) when $R_0 < 1$.

Appendix C. Existence conditions for the disease-induced hydra effect

Recall the assumption that reduction in reproduction and resource competition for infectious individuals are the same, denoted by τ . Infectious diseases may completely unaffect ($\tau=1$), completely inhibit ($\tau=0$) or partially inhibit ($\tau\in(0,1)$) recruitment. Here, we discuss the existence of the disease-induced hydra effect and the sufficient conditions required for its existence in each of the above three cases. Note that the unique endemic equilibrium (S^* , I^*) exists if the basic reproduction number $R_0>1$, where $R_0=\beta S_0/(d+\alpha+\gamma)$. Denote $N^*=S^*+I^*$. For the first case ($\tau=1$), we have

$$bN^*F(N^*) = dN^* + \alpha I^* > dN^* = bF(S_0)N^* \Rightarrow F(N^*) > F(S_0).$$

Since F(x) is a monotonically decreasing function, we obtain $N^* < S_0$. This implies that there is no disease-induced hydra effect in system (1) when $\tau = 1$.

For the second case ($\tau = 0$), simple calculation yields

$$N^* = \frac{S^*(bF(S^*) + \alpha)}{d + \alpha} \text{ and } \frac{\partial S^*}{\partial R_0} = -\frac{S_0}{R_0^2}.$$

Differentiating N^* with respect to R_0 gives

$$\partial N^*/\partial R_0 > 0 \Leftrightarrow \frac{d}{dS^*}[S^*F(S^*)] < -\frac{\alpha}{b}.$$

This implies that the existence of disease-induced hydra effect requires an overcompensatory recruitment; i.e., $\frac{d}{dS}(bSF(S)) < 0$ for some interval (Jaramillo et al. 2022). It is easy to verify that the resource competition among hosts in epidemiological model (1) yields overcompensatory recruitment. That is, the disease-induced hydra effect could occur in system (1) when $\tau = 0$.

Next, we consider the third case $(\tau \in (0, 1))$. Recall that we want conditions where the endemic equilibrium is greater than the disease-free equilibrium; i.e., $N^* > S_0$ when $R_0 > 1$. Thus, we want $2\tau^2 bq S^* + (b\tau(1-2qS^*) - \alpha - d + \sqrt{\Delta}) > 2\tau^2(b-d)$,



where $\triangle = (b\tau(1-2qS^*)-\alpha-d)^2+4b\tau^2q(bS^*(1-qS^*)-dS^*)>0$. For this inequality to hold, it is sufficient to have

$$2(bqS^* - b + d)\tau^2 + b(1 - 2qS^*)\tau - (\alpha + d) > 0.$$
(6)

We can verify that the left-hand side of inequality (6) is a downward-facing quadratic function when $R_0 > 1$ ($bqS^* - b + d < 0$). This shows that inequality (6) may hold only if the downward-facing quadratic function has two eigenvalues with $\tau_b < \tau_t < 1$ and $\tau_t > 0$. That is, we need to restrict $\bar{\Delta} = b^2(1 - 2qS^*)^2 + 8(\alpha + d)(bqS^* - b + d) > 0$. The interval of validity is $\tau \in (\max\{0, \tau_b\}, \tau_t)$. Further, we can verify that $\tau_t < 0$ when $2qS^* > 1$. Thus, we need to constrain $2qS^* \le 1$. Simple calculation gives

$$\tau_t = \frac{b(1 - 2qS^*) + \sqrt{\bar{\Delta}}}{4(b - d - bqS^*)} > 0, \ \tau_b = \frac{b(1 - 2qS^*) - \sqrt{\bar{\Delta}}}{4(b - d - bqS^*)}.$$

When $2qS^*=1$, the interval of validity is $\tau \in (0, \tau_t)$; when $2qS^*<1$, the interval of validity is $\tau \in (\tau_b, \tau_t)$. Note that we need 2d < b to ensure that $\tau_t < 1$. Sufficient conditions for the existence of the disease-induced hydra effect in epidemic system (1) are summarized in Theorem 3.

Appendix D. Invasion fitness of mutant host and mutant pathogen

To analyze the dynamic process of co-evolution, we assume for the sake of simplicity that mutations are minor and rare and that the host and pathogen cannot mutate simultaneously. The basic reproduction number R_0 represents the expected number of secondary cases produced by a typical infected individual during his/her infectious period in a fully susceptible population. For pathogens, the goal is to maximize their population size, which at the macro level translates to infecting as many individuals as possible. Therefore, using R_0 as the fitness for the pathogen is appropriate. For the host (including both susceptible and infected individuals), fitness must account for both groups rather than just the susceptible population. Thus, we use expected lifetime reproductive success (ELRS) as the fitness for the host. ELRS quantifies the expected number of offspring that the host (both susceptible and infected) can produce over their lifetime, making it a reasonable choice for host fitness.

First, we consider the presence of mutant hosts. Note that the host fitness function must include two reproductive phases: uninfected and infected. Consider the mutant host with traits $(b(x_m), \alpha(x_m, y), \beta(x_m, y))$ that tries to invade the resident host $(b(x), \alpha(x, y), \beta(x, y))$ set at its equilibrium $(S^*(x, y), I^*(x, y))$. The mutant dynamics are given by the system

$$\frac{dS_m}{dt} = b(x_m)(S_m + \tau I_m)F(S^*(x, y) + \tau I^*(x, y)) - \beta(x_m, y)S_m I^*(x, y) - dS_m + \gamma I_m,
\frac{dI_m}{dt} = \beta(x_m, y)S_m I^*(x, y) - (\alpha(x_m, y) + d + \gamma)I_m.$$



148 Page 24 of 28 Q. Liu et al.

Let $p_S(t)$ and $p_I(t)$ be the respective probabilities of remaining in the uninfected and infected states; i.e., the proportions of uninfected and infected mutant hosts relative to the initial mutant host density at time t (Baalen 1998). Further, we have

$$\frac{d\vec{p}}{dt} = A_m \vec{p}(t),$$

where

$$A_m = \begin{pmatrix} -\beta(x_m, y)I^*(x, y) - d & \gamma \\ \beta(x_m, y)I^*(x, y) & -d - \alpha(x_m, y) - \gamma \end{pmatrix},$$

$$\vec{p}(t) = \begin{pmatrix} p_S(t) \\ p_I(t) \end{pmatrix} \text{ and } \vec{p}(0) = \begin{pmatrix} 1 \\ 0 \end{pmatrix}.$$

The expected time spent in either state is given by the following expression:

$$\int_{0}^{\infty} \vec{p}(t)dt = -A_{m}^{-1} \cdot \vec{p}(0), \tag{7}$$

which sum to the expected longevity of the host (Baalen 1998). Note that the birth rate vector \vec{b}_m is given by

$$\vec{b}_m = (b(x_m)F(S^*(x, y) + \tau I^*(x, y)) \quad \tau b(x_m)F(S^*(x, y) + \tau I^*(x, y)))^T.$$

The mutant host fitness $f_1(x_m, x, y)$ is defined as the scalar product of vector (7) and the vector of birth rates \vec{b}_m . If $f_1(x_m, x, y) > 1$, the population density of the mutant host will increase, and we claim that the mutant host can invade. It is easy to verify that $f_1(x_m, x, y) |_{x_m = x} = f_1(x, x, y) = f_1(x, y) = 1$.

Next, suppose a mutant pathogen with different virulence y_m enters into the resident community at low density. Denote the individual infected by the mutant pathogen as I_m . The resident-mutant population dynamics becomes

$$\frac{dS}{dt} = b(x)(S + \tau I + \tau I_m)F(S + \tau I + \tau I_m)
- (\beta(x, y)I + \beta(x, y_m)I_m)S - dS + \gamma(I + I_m),
\frac{dI}{dt} = \beta(x, y)SI - \alpha(x, y)I - dI - \gamma I,
\frac{dI_m}{dt} = \beta(x, y_m)SI_m - \alpha(x, y_m)I_m - dI_m - \gamma I_m.$$
(8)

The stability of the boundary equilibrium $E_b(S^*(x, y), I^*(x, y), 0)$ determines whether the mutant pathogen can successfully invade or not (Yang et al. 2022). The Jacobian matrix associated with the linearization for model (8) at E_b is

$$J(E_b) = \begin{pmatrix} J_{res} & J_{12} \\ \vec{0} & J_{mut} \end{pmatrix},$$



where

$$\begin{split} J_{res} &= \begin{pmatrix} b(x)(1-2q(S+\tau I)) - \beta(x,y)I - d \ \tau b(x)(1-2q(S+\tau I)) - \beta(x,y)S + \gamma \\ \beta(x,y)I & \beta(x,y)S - \alpha(x,y) - d - \gamma \end{pmatrix}, \\ J_{12} &= (\tau b(x)(1-2q(S+\tau I)) - \beta(x,y_m)S + \gamma, \ 0)^T, \ \vec{0} = (0,\ 0), \\ J_{mut} &= \beta(x,y_m)S^*(x,y) - d - \alpha(x,y_m) - \gamma. \end{split}$$

Since the endemic equilibrium $(S^*(x, y), I^*(x, y))$ of model (1) is asymptotically stable, the local stability of E_b is determined by the single eigenvalue of J_{mut} . If $J_{mut} > 0$, then the population density of mutant pathogen will increase. Note that the expected number of secondary cases produced by a single host infected by this mutant over its entire infectious period (Gandon et al. 2001) is given by

$$R_0[y_m, x, y] = \frac{\beta(x, y_m)S^*(x, y)}{d + \alpha(x, y_m) + \gamma}.$$

Since $J_{mut} > 0 \Leftrightarrow R_0[y_m, x, y] > 1$, the mutant pathogen fitness $f_2(y_m, x, y)$ is then defined as $R_0[y_m, x, y]$. If $f_2(y_m, x, y) > 1$, we claim that the mutant pathogen can invade. Simple calculation yields $f_2(y_m, x, y)|_{y_m=y} = f_2(y, x, y) = f_2(x, y) = 1$.

Appendix E. The invasion fitness of resistance and tolerance

For simplicity, we assume that the pathogen virulence has reached the evolutionary endpoint (CSS, $y = y^*$ fixed). If host defense refers to resistance only and we restrict the scope to avoidance case — i.e., host resistance results in reduced transmission rates — the trade-off functions become $b(x^r)$, $\beta(x^r, y)$ and $\alpha(y)$. Epidemiologically, the non-negative trade-off functions satisfy (H1), (H3) and $\alpha'(y) > 0$ for all $x^r, y \in \mathbb{C}$.. The invasion fitness for the mutant host is

$$f_r(x_m^r, x^r, y) = \frac{b(x_m^r)(d + \alpha(y) + \gamma + \beta(x_m^r, y)I^*(x^r, y)\tau)F(S^*(x^r, y) + \tau I^*(x^r, y))}{(d + \beta(x_m^r, y)I^*(x^r, y))(d + \alpha(y) + \gamma) - \beta(x_m^r, y)I^*(x^r, y)\gamma}.$$

Similarly, if the host defense refers to tolerance only, the trade-off functions become $b(x^t)$, $\beta(y)$ and $\alpha(x^t, y)$, which satisfy (H1)–(H2) and $\beta'(y) > 0$ for all $x^r, y \in \mathbb{C}$.. The invasion fitness for the mutant host is

$$f_t(x_m^t, x^t, y) = \frac{b(x_m^t)(d + \alpha(x_m^t, y) + \gamma + \beta(y)I^*(x^t, y)\tau)F(S^*(x^t, y) + \tau I^*(x^t, y))}{(d + \beta(y)I^*(x^t, y))(d + \alpha(x_m^t, y) + \gamma) - \beta(y)I^*(x^t, y)\gamma}.$$

The evolutionary dynamics of host traits (x_r, x_t) is given by

$$\frac{dx^r}{dT} \approx \mu_r g_r(x^r, y),$$

$$\frac{dx^t}{dT} \approx \mu_t g_t(x^t, y),$$



148 Page 26 of 28 Q. Liu et al.

where

$$g_r(x^r,y) = \frac{\partial f_r(x_m^r,x^r,y)}{\partial x_m^r} \bigg|_{x_m^r = x^r}, \ g_t(x^t,y) = \frac{\partial f_t(x_m^t,x^t,y)}{\partial x_m^t} \bigg|_{x_m^t = x^t}.$$

For the next step, we need to consider pure and combined host-defense strategies in the context of host-pathogen co-evolution. We leave these for future work.

Acknowledgements QL was a recipient of Chinese Scholarship Council (CSC) funding. SS? is supported by an NSERC Discovery Grant. For citation purposes, please note that the question mark in "Smith?" is part of her name.

Funding YX is supported by National Natural Science Foundation of China (12220101001, 12031010).

References

Aiewsakun P, Katzourakis A (2016) Time-dependent rate phenomenon in viruses. J Virol 90(16):7184–7195 Alizon S, Hurford A, Mideo N, Van Baalen M (2009) Virulence evolution and the trade-off hypothesis: history, current state of affairs and the future. J Evol Biol 22(2):245–259

Anderson RM, May RM (1981) The population dynamics of microparasites and their invertebrate hosts, Philosophical Transactions of the Royal Society of London. B Biological Sciences 291(1054):451–524

Antonovics J, Thrall PH (1994) The cost of resistance and the maintenance of genetic polymorphism in host-pathogen systems, Proceedings of the Royal Society of London. Series B Biological Sciences 257(1349):105–110

Ashby B, Boots M (2015) Coevolution of parasite virulence and host mating strategies. Proc Natl Acad Sci 112(43):13290–13295

Ashby B, Iritani R, Best A, White A, Boots M (2019) Understanding the role of eco-evolutionary feedbacks in host-parasite coevolution. J Theor Biol 464:115–125

Baalen MV (1998) Coevolution of recovery ability and virulence, Proceedings of the Royal Society of London. Series B Biological Sciences 265(1393):317–325

Bartlett LJ, Wilfert L, Boots M (2018) A genotypic trade-off between constitutive resistance to viral infection and host growth rate. Evolution 72(12):2749–2757

Best A, White A, Boots M (2009) The implications of coevolutionary dynamics to host-parasite interactions. Am Nat 173(6):779–791

Best A, Webb S, White A, Boots M (2011) Host resistance and coevolution in spatially structured populations. Proceedings of the Royal Society B Biological Sciences 278(1715):2216–2222

Best A, Bowers R, White A (2015) Evolution, the loss of diversity and the role of trade-offs. Math Biosci 264:86-93

Best A, White A, Boots M (2017) The evolution of host defence when parasites impact reprodution. Evol Ecol Res 18:393–409

Boldin B, Diekmann O (2008) Superinfections can induce evolutionarily stable coexistence of pathogens. J Math Biol 56:635–672

Bonachela JA (2024) Viral plasticity facilitates host diversity in challenging environments. Nat Commun 15(1):7473

Bonneaud C, Longdon B (2020) Emerging pathogen evolution: Using evolutionary theory to understand the fate of novel infectious pathogens. EMBO Rep 21(9):e51374

Bonneaud C, Tardy L, Giraudeau M, Hill GE, McGraw KJ, Wilson AJ (2019) Evolution of both host resistance and tolerance to an emerging bacterial pathogen. Evolution Letters 3(5):544–554

Boots M, Bowers RG (1999) Three mechanisms of host resistance to microparasites-avoidance, recovery and tolerance-show different evolutionary dynamics. J Theor Biol 201(1):13–23

Boots M, Best A, Miller MR, White A (2009) The role of ecological feedbacks in the evolution of host defence: what does theory tell us? Philosophical Transactions of the Royal Society B Biological Sciences 364(1513):27–36

Buckingham LJ, Ashby B (2022) Coevolutionary theory of hosts and parasites. J Evol Biol 35(2):205-224



- Bull JJ, Lauring AS (2014) Theory and empiricism in virulence evolution. PLoS Pathog 10(10):e1004387 Carmona D, Fornoni J (2013) Herbivores can select for mixed defensive strategies in plants. New Phytol 197(2):576–585
- Castledine M, Padfield D, Sierocinski P, Pascual JS, Hughes A, Mäkinen L, Friman V-P, Pirnay J-P, Merabishvili M, De Vos D et al (2022) Parallel evolution of pseudomonas aeruginosa phage resistance and virulence loss in response to phage treatment in vivo and in vitro. Elife 11:e73679
- Christiansen FB (1991) On conditions for evolutionary stability for a continuously varying character. Am Nat 138(1):37–50
- Cressler CE, Graham AL, Day T (2015) Evolution of hosts paying manifold costs of defence. Proceedings of the Royal Society B Biological Sciences 282(1804):20150065
- Cressman R (2010) CSS, NIS and dynamic stability for two-species behavioral models with continuous trait spaces. J Theor Biol 262(1):80–89
- Day T, Kennedy DA, Read AF, Gandon S (2022) Pathogen evolution during vaccination campaigns. PLoS Biol 20(9):e3001804
- Decaestecker E, Gaba S, Raeymaekers JA, Stoks R, Van Kerckhoven L, Ebert D, De Meester L (2007) Host-parasite 'Red Queen'dynamics archived in pond sediment. Nature 450(7171):870–873
- Dieckmann U, Law R (1996) The dynamical theory of coevolution: a derivation from stochastic ecological processes. J Math Biol 34:579–612
- Doumayrou J, Avellan A, Froissart R, Michalakis Y (2013) An experimental test of the transmission-virulence trade-off hypothesis in a plant virus. Evolution 67(2):477–486
- Duffy S, Shackelton LA, Holmes EC (2008) Rates of evolutionary change in viruses: patterns and determinants. Nat Rev Genet 9(4):267–276
- F. Dumortier, J. Llibre, J. C. Artés, Qualitative theory of planar differential systems, Vol. 2, Springer, 2006 Gandon S, Mackinnon MJ, Nee S, Read AF (2001) Imperfect vaccines and the evolution of pathogen virulence. Nature 414(6865):751–756
- Gandon S, Mackinnon M, Nee S, Read A (2003) Imperfect vaccination: some epidemiological and evolutionary consequences, Proceedings of the Royal Society of London. Series B Biological Sciences 270(1520):1129–1136
- Gascuel F, Choisy M, Duplantier J-M, Débarre F, Brouat C (2013) Host resistance, population structure and the long-term persistence of bubonic plague: contributions of a modelling approach in the malagasy focus. PLoS Comput Biol 9(5):e1003039
- Geritz SA, Kisdi E, Mesze' NA G, Metz JA (1998) Evolutionarily singular strategies and the adaptive growth and branching of the evolutionary tree. Evol Ecol 12:35–57
- Geritz SA, Gyllenberg M, Jacobs FJ, Parvinen K (2002) Invasion dynamics and attractor inheritance. J Math Biol 44:548–560
- Gómez P, Buckling A (2011) Bacteria-phage antagonistic coevolution in soil. Science 332(6025):106–109
 Hall AR, Scanlan PD, Morgan AD, Buckling A (2011) Host-parasite coevolutionary arms races give way to fluctuating selection. Ecol Lett 14(7):635–642
- Heffernan JM, Smith RJ, Wahl LM (2005) Perspectives on the basic reproductive ratio. J R Soc Interface 2(4):281–293
- Hulse SV, Antonovics J, Hood ME, Bruns EL (2023) Specific resistance prevents the evolution of general resistance and facilitates disease emergence. J Evol Biol 36(5):753–763
- Hulse SV, Antonovics J, Hood ME, Bruns EL (2023) Host-pathogen coevolution promotes the evolution of general, broad-spectrum resistance and reduces foreign pathogen spillover risk. Evolution Letters 7(6):467–477
- Iwasa Y, Pomiankowski A, Nee S (1991) The evolution of costly mate preferences II. The "handicap" principle Evolution 45(6):1431–1442
- Jaramillo J, Ma J, van den Driessche P, Yakubu A-A (2022) Disease-induced hydra effect with overcompensatory recruitment. Bull Math Biol 84(1):17
- Kisdi E (1999) Evolutionary branching under asymmetric competition. J Theor Biol 197(2):149–162
- Kun Á, Hubai AG, Král A, Mokos J, Mikulecz BÁ, Radványi Á (2023) Do pathogens always evolve to be less virulent? the virulence-transmission trade-off in light of the covid-19 pandemic. Biologia futura 74(1):69–80
- Liu Q, Xiao Y (2023) A coupled evolutionary model of the viral virulence in an SIS community. Discrete and Continuous Dynamical Systems-B 28(9):5012–5036
- Liu J, Gefen O, Ronin I, Bar-Meir M, Balaban NQ (2020) Effect of tolerance on the evolution of antibiotic resistance under drug combinations. Science 367(6474):200–204



148 Page 28 of 28 Q. Liu et al.

Lopez-pascua DC, Buckling A (2008) Increasing productivity accelerates host-parasite coevolution. J Evol Biol 21(3):853–860

- Malo D, Skamene E (1994) Genetic control of host resistance to infection. Trends Genet 10(10):365-371
- McCallum M, Czudnochowski N, Rosen LE, Zepeda SK, Bowen JE, Walls AC, Hauser K, Joshi A, Stewart C, Dillen JR et al (2022) Structural basis of SARS-CoV-2 Omicron immune evasion and receptor engagement. Science 375(6583):864–868
- McCarville J, Ayres J (2018) Disease tolerance: concept and mechanisms. Curr Opin Immunol 50:88–93
- McLeod DV, Day T (2015) Pathogen evolution under host avoidance plasticity. Proceedings of the Royal Society B Biological Sciences 282(1814):20151656
- Metz JA, Nisbet RM, Geritz SA (1992) How should we define 'fitness' for general ecological scenarios? Trends in ecology & evolution 7(6):198–202
- Miller MR, White A, Boots M (2007) Host life span and the evolution of resistance characteristics. Evolution 61(1):2–14
- Mougi A, Iwasa Y (2010) Evolution towards oscillation or stability in a predator-prey system. Proceedings of the Royal Society B Biological Sciences 277(1697):3163–3171
- Nuismer SL, Ridenhour BJ, Oswald BP (2007) Antagonistic coevolution mediated by phenotypic differences between quantitative traits. Evolution 61(8):1823–1834
- Núñez-Farfán J, Fornoni J, Valverde PL (2007) The evolution of resistance and tolerance to herbivores. Annu Rev Ecol Evol Syst 38(1):541–566
- Pechous RD, Sivaraman V, Stasulli NM, Goldman WE (2016) Pneumonic plague: the darker side of yersinia pestis. Trends Microbiol 24(3):190–197
- Post DM, Palkovacs EP (2009) Eco-evolutionary feedbacks in community and ecosystem ecology: interactions between the ecological theatre and the evolutionary play. Philosophical Transactions of the Royal Society B Biological Sciences 364(1523):1629–1640
- Restif O, Koella JC (2004) Concurrent evolution of resistance and tolerance to pathogens. Am Nat 164(4):E90-E102
- Simmonds P, Aiewsakun P, Katzourakis A (2019) Prisoners of war-host adaptation and its constraints on virus evolution. Nat Rev Microbiol 17(5):321–328
- Singh P, Best A (2021) Simultaneous evolution of host resistance and tolerance to parasitism. J Evol Biol 34(12):1932–1943
- Singh P, Best A (2023) A sterility-mortality tolerance trade-off leads to within-population variation in host tolerance. Bull Math Biol 85(3):16
- J. M. Smith, Evolution and the Theory of Games, Cambridge university press, 1982
- Stowe KA (1998) Experimental evolution of resistance in brassica rapa: correlated response of tolerance in lines selected for glucosinolate content. Evolution 52(3):703–712
- M. Tibayrenc, Genetics and evolution of infectious diseases, Elsevier, 2024
- Vitale C, Best A (2019) The paradox of tolerance: parasite extinction due to the evolution of host defence. J Theor Biol 474:78–87
- Wakano JY, Iwasa Y (2013) Evolutionary branching in a finite population: deterministic branching vs. stochastic branching. Genetics 193(1):229–241
- Woolhouse ME, Webster JP, Domingo E, Charlesworth B, Levin BR (2002) Biological and biomedical implications of the co-evolution of pathogens and their hosts. Nat Genet 32(4):569–577
- Yang Y, Ma C, Zu J (2022) Coevolutionary dynamics of host-pathogen interaction with density-dependent mortality. J Math Biol 85(2):15
- Zu J, Wang K, Mimura M (2011) Evolutionary branching and evolutionarily stable coexistence of predator species: Critical function analysis. Math Biosci 231(2):210–224
- Zu J, Li M, Gu Y, Fu S (2020) Modelling the evolutionary dynamics of host resistance-related traits in a susceptible-infected community with density-dependent mortality. Discrete and Continuous Dynamical Systems-B 25(8):3049–3086

Publisher's Note Springer Nature remains neutral with regard to jurisdictional claims in published maps and institutional affiliations.

Springer Nature or its licensor (e.g. a society or other partner) holds exclusive rights to this article under a publishing agreement with the author(s) or other rightsholder(s); author self-archiving of the accepted manuscript version of this article is solely governed by the terms of such publishing agreement and applicable law.

